Novel multi-drugs incorporating hybrid-structured nanofibers enhance alkylating agent activity in malignant gliomas

Ther Adv Med Oncol

2019, Vol. 11: 1–17

DOI: 10.1177/1758835919875555

Shih-Jung Liu, Shun-Tai Yang, Shu-Mei Chen, Yin-Chen Huang, Wei-Hwa Lee, Jui Ho, Yin-Chun Chen and Yuan-Yun Tseng

Abstract

Background: Malignant gliomas (MGs) are highly chemotherapy-resistant. Temozolomide (TMZ) and carmustine (BiCNU) are alkylating agents clinically used for treating MGs. However, their effectiveness is restrained by overexpression of the DNA repair protein O^6-methylguanine-DNA methyltransferase (MGMT) in tumors. O^6-benzylguanine (O^6-BG) is a nonreversible inhibitor of MGMT, it promotes the cytotoxicity of alkylating chemotherapy. The authors have developed a hybrid-structured nanofibrous membrane (HSNM) that sequentially delivers high concentrations of O^6-BG, BiCNU, and TMZ in an attempt to provide an alternative to the current therapeutic options for MGs.

Methods: The HSNMs were implanted onto the cerebral surface of pathogen-free rats following surgical craniectomy, while the *in vivo* release behaviors of O^6-BG, TMZ, and BiCNU from the HSNMs were explored. Subsequently, the HSNMs were surgically implanted onto the brain surface of two types of tumor-bearing rats. The survival rate, tumor volume, malignancy of tumor, and apoptotic cell death were evaluated and compared with other treatment regimens.

Results: The biodegradable HSNMs sequentially and sustainably delivered high concentrations of O^6-BG, BiCNU, and TMZ for more than 14 weeks. The tumor-bearing rats treated with HSNMs demonstrated therapeutic advantages in terms of retarded and restricted tumor growth, prolonged survival time, and attenuated malignancy.

Conclusion: The results demonstrated that O^6-BG potentiates the effects of interstitially transported BiCNU and TMZ. Therefore, O^6-BG may be required for alkylating agents to offer maximum therapeutic benefits for the treatment of MGMT-expressing tumors. In addition, the HSNM-supported chemoprotective gene therapy enhanced chemotherapy tolerance and efficacy. It can, therefore, potentially provide an improved therapeutic alternative for MGs.

Keywords: chemoresistance, malignant glioma, nanofibrous membrane, O^6-benzylguanine (O^6-BG), O^6-methylguanine-DNA methyltransferase (MGMT)

Received: 4 December 2018; revised manuscript accepted: 19 August 2019.

Correspondence to:
Yuan-Yun Tseng
Division of Neurosurgery, Department of Surgery, Shuang Ho Hospital, Taipei Medical University, No. 291, Zhongzheng Rd., Zhonghe Dist., Taipei, 235

Department of Surgery, School of Medicine, College of Medicine, Taipei Medical University, Taipei
britsey@gmail.com

Shih-Jung Liu
Department of Mechanical Engineering, Chang Gung University, Tao-Yuan

Department of Orthopedic Surgery, Chang Gung Memorial Hospital-Linkuo, Tao-Yuan

Shun-Tai Yang
Division of Neurosurgery, Department of Surgery, Shuang Ho Hospital, Taipei Medical University, Taipei

Department of Surgery, School of Medicine, College of Medicine, Taipei Medical University, Taipei

Shu-Mei Chen
Division of Neurosurgery, Department of Surgery, Shuang Ho Hospital, Taipei Medical University, Taipei

Department of Neurosurgery, Wan Fang Hospital, Taipei Medical University, Taipei

Yin-Chen Huang
Department of Neurosurgery, Chang Gung Memorial Hospital-Linkuo, Chang Gung University College of Medicine, Tao-Yuan

Wei-Hwa Lee
Department of Pathology, Shuang Ho Hospital, Taipei Medical University, Taipei

Jui Ho

Yin-Chun Chen
Department of Mechanical Engineering, Chang Gung University, Tao-Yuan

Introduction

Malignant glioma (MG) is the most aggressive and common type of adult brain tumor, with a relatively low overall survival rate and limited treatment options.[1–3] These tumors are currently treated with extreme surgical debulking and external radiation therapy. Despite multimode therapy for patients with newly diagnosed MG, the median survival rate remains approximately 14.6 months. In addition, recurrent MG has a poor prognosis, with a 6 month progression-free survival rate of 15–21% and a median survival of 15 weeks.[2] Although surgical resection can effectively reduce tumor size and mass, maximal surgical resection is frequently required to achieve improved overall survival.[3] However, considering their aggressive infiltrating nature, an entire neurosurgical excision of these tumors is not possible.

However, survival can be further extended by including the alkylating agents, temozolomide (TMZ) and carmustine (BiCNU), in the therapeutic regimen. Although concomitant TMZ and radiotherapy abided by adjuvant TMZ remains the current norm of treatment, the median survival of patients with MG is approximately 12–16 months.[4–6] Considering the location of the MG tumor, the passage of pharmaceuticals through the blood-brain barrier (BBB) and within the tumor remains poor. In addition, a number of factors contribute to the poor prognosis of MG. These include the development of tumor resistance to chemotherapy and radiotherapy, the extremely infiltrative ability as well as genetic, molecular, and morphological heterogeneity of the tumor cells, and the highly developed but inadequately functioning neovasculature.[7–9]

Although TMZ, an oral alkylating agent, is widely employed to treat MG, over 50% of patients treated with TMZ do not respond. TMZ incurs DNA methylation of guanine at the O^6-position, making O^6-methylguanine incorrectly pair with thymine, this results in the mismatch repair system and leads to a double-strand break of the genome. This leads to cell cycle arrest at the G2/M phase and eventually apoptosis.[10,11] Furthermore, BiCNU exerts tumoricidal effects through DNA chloroethylation, also at the O^6-position of guanine.[12] O^6-methylguanine-DNA methyltransferase (MGMT) protects the tumors from this damage by eliminating DNA adduction from the O^6-position before cytotoxic interstrand crosslinking occurs.[11–13] Researchers have studied MGMT inhibition combined with a chemotherapeutic alkylating agent to improve MG treatment clinically. O^6-benzylguanine (O^6-BG) is a low-molecular-weight pseudosubstrate that transmits a benzyl group to the MGMT-active-site cysteine-145 residue, thus irreversibly inactivating MGMT and preventing the eradication of the methyl group from DNA.[14] O^6-BG is inert and nontoxic when used alone, but is an effective inhibitor of MGMT in combination with alkylating agents. In animal models with MGMT-active (nonmethylated) BiCNU-resistant tumors, the bioactivity of MGMT was suppressed for several hours following pretreatment of O^6-BG.[15] Similarly, MGMT-deficient human central nervous system tumor xenografts were more sensitive to alkylating agents than to MGMT alone.[16,17]

Systemic BiCNU is effective against MG, but has high toxicity, limiting its clinical use.[18,19] The majority of MGs regrow within 2–3 cm of the primitive excision location and inside the radiation area.[20] Polifeprosan 20 with a BiCNU transplant (Gliadel wafer; Guilford Pharmaceuticals, Baltimore, MD) conveys BiCNU locally to the tumor location with no local or systemic adverse side effects.[20,21]

In this study, the authors embedded O^6-BG into the core of a novel core-sheath structured 50:50 poly[(d,l)-lactide-co-glycolide] (PLGA) nanofibers by adopting coaxial electrospinning techniques. Subsequently the authors loaded two alkylating agents (BiCNU and TMZ) into blended 75:25 PLGA nanofibers using customary electrospinning techniques to obtain biodegradable hybrid bilayer-structured nanofibrous membranes (HSNMs). The HSNMs were implanted onto the cerebral surface of pathogen-free rats following surgical craniectomy, while the *in vivo* release behaviors of O^6-BG, TMZ, and BiCNU from the HSNMs were explored. Subsequently, the HSNMs were transplanted onto the cerebral surface of animals bearing tumors of two cell lines, F98 and 9L. Based on the cell line, the rats received one of the following treatment regimens: oral TMZ with Gliadel wafer implant, single-layer nanofibrous membrane implant loaded with BiCNU and TMZ, pretreatment with intraperitoneal O^6-BG, followed by a Gliadel wafer implant and oral TMZ, HSNM implantation, or no treatment. The authors assessed changes in the gross wound appearance and tumor volume (TV) through serial brain magnetic resonance imaging (MRI) and performed survival analysis and histological examination, including hematoxylin and eosin (H&E) staining, Ki-67 labeling index, and glial fibrillary acidic protein expression (GFAP). In addition, the therapeutic efficacies of the various regimens were compared and evaluated.

Materials and methods

HSNM fabrication

Two structured nanofibers were prepared: a core-sheath O^6-BG on 50:50 PLGA nanofibers and blended alkylating agents (TMZ and BiCNU) on 75:25 PLGA nanofibers. Core-sheath nanofibers were fabricated using a coaxial spinning device that transports two solutions simultaneously. Preset percentages of 50:50 PLGA (240 mg) were dissolved in 1 ml of hexafluoroisopropanol (HFIP; Sigma Aldrich, USA), in addition, 10 mg of O^6-BG was dissolved in 1 ml of methanol.

Then the 50:50 PLGA and O^6-BG solutions were placed into two individual syringes for coaxial electrospinning. During the spinning process, the solutions were conveyed by two individually controlled pumps at flowrates of 0.3 and 0.9 ml/h for the core O^6-BG and sheath PLGA solutions, respectively. The solutions in the syringe were subjected to a voltage of +15 kV, and the collecting aluminum sheet was 15 cm away from the needle tip.

Then, 1 ml of HFIP was used to dissolve the 75:25 PLGA (250 mg) and alkylating agents (20 mg TMZ and 20 mg BiCNU). The solution was transported and then spun at ambient temperature using a syringe pump. The flow rate of the pump was 1.8 ml/h. The same aluminum sheet was used to gather the spun nanofibers in a nonwoven shape. Hybrid bilayer nanofibrous membranes with two structures, namely core-sheath and blend nanofibers, were obtained with a thickness of approximately 0.12 mm.

Chemicals and reagents

Lactide:glycolide, 50:50 and 75:25 poly(lactide-co-glycolide) polymers (Resomer RG503 and RG756, respectively), and O^6-BG, BiCNU, and TMZ were all purchased from Sigma Aldrich (Mo, USA). An oral TMZ, Temodal 100 mh, was purchased from Lotus Pharm. Co. (Taipei, Taiwan).

Characterization of prepared HSNMs

To evaluate the nanofiber size distribution, the morphology of electrospun nanofibers was observed on a scanning electron microscope (SEM) (JEOL Model JSM-7500F, Japan) after they were coated with gold. The diameter distribution was acquired by analyzing SEM images of 100 randomly chosen fibers for each test specimen ($n = 3$) utilizing a commercial Image J image software (National Institutes of Health, Bethesda, MD, USA). In addition, to verify the incorporation of pharmaceuticals into the HSNM, Fourier transform infrared (FTIR) analysis was conducted using a Bruker Tensor 27 spectrophotometer at a resolution of 4 cm^{-1} and 32 scans. All samples were depressed as KBr disks and analyzed from 400 to 4000 cm^{-1}.

Animals and tumor cells

Pathogen-free, male Fischer 344 rats ($n = 150$), weighing 250–300 g, were purchased from BioLASCO Taiwan Co. Ltd. (Taipei, Taiwan). The rats were quarantined in the animal center for 7 days prior to use. All experimental procedures involving animals received Institutional Animal Care and Use Committee approval (LAC-2015-0157) from Taipei Medical University. All of the studied animals were cared for in a manner consistent with the regulations of the Ministry of Health and Welfare, Taiwan under the supervision of a licensed veterinarian. All procedures were designed to minimize the suffering and number of animals in compliance with ethical standards of the institution of the national research committee. The rat MG cell line F98 (ATCC-CRL-2948) and gliosarcoma cell line 9L (ATCC-CRL-2200) were purchased from American Type Culture Collection. All cell lines were cultured in Dulbecco's Modified Essential Medium (Wako) supplemented with 10% fetal bovine serum.

Cell lysate preparation and immunoblotting

Cell pellets were suspended in RIPA buffer [150 mM NaCl, 1 mM EDTA, 1% nonidet P-40, 0.5% sodium deoxycholate, 0.1% sodium dodecyl sulfate (SDS), and 50 mM Tris–HCl] supplemented with protease inhibitors and phosphatase inhibitors. Cell lysates were prepared following homogenization and were centrifuged at 14,000 rpm at 4°C for 15 min. Total proteins were separated employing 8–12% SDS polyacrylamide gel electrophoresis and transferred to nitrocellulose membranes (Millipore). Nonspecific binding on membranes was blocked by 5% nonfat milk in tris-buffered saline and polysorbate 20 (TBST) including 10 mM of Tris–HCl, pH 7.4, 150 nM NaCl, and 0.01% (v/v) Tween 20 for 1 h. Subsequently, the membranes were washed with TBST and respectively hybridized with antibodies against MGMT and GAPDH (Santa Cruz Biotechnology) at 4°C overnight. After washing with TBST, the membranes were incubated with goat antimouse-IgG coupled to horseradish peroxidase (Santa Cruz Biotechnology) at room temperature for 2 h. Finally, the detection was completed using enhanced chemiluminescence substrate (Millipore). Densitometric analysis (Image J) was employed to reveal relative band intensities normalized to levels of GAPDH.

Intracranial tumor implantation

The authors anesthetized 150 rats using an intraperitoneal injection of 6% chloral hydrate (6 ml/

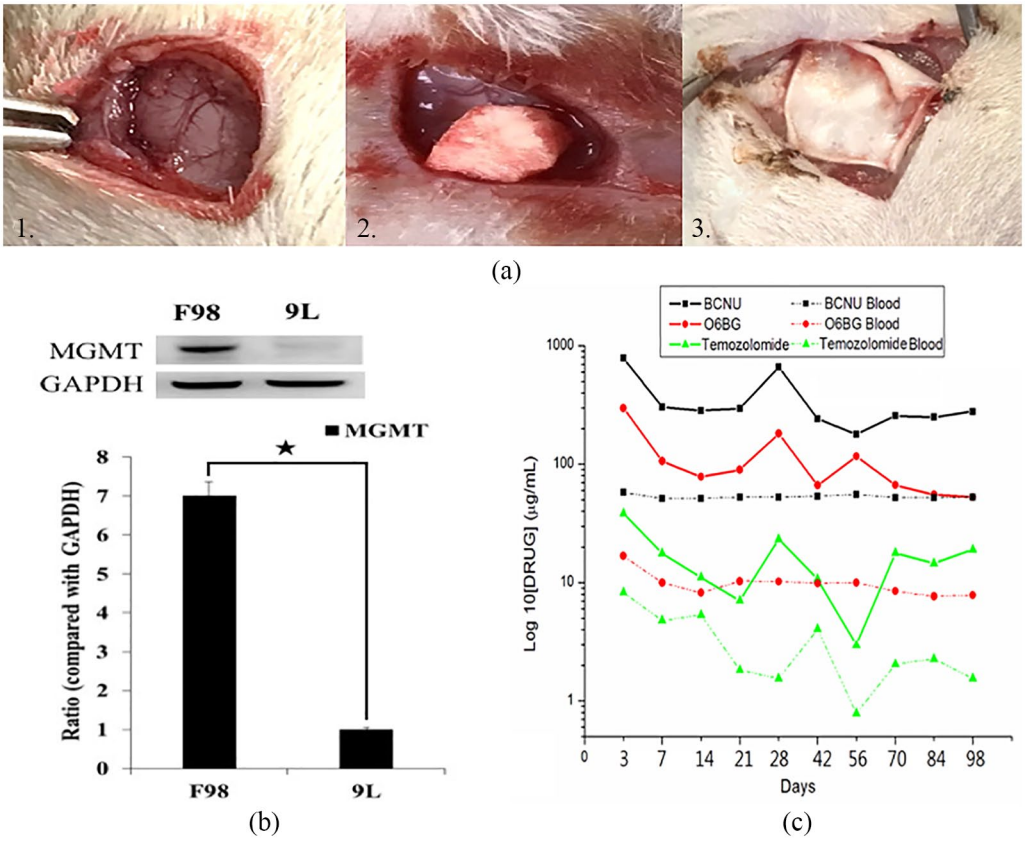

Figure 1. The surgical procedure, tumor cell, and *in vivo* drug study. (a) 1. Craniectomy (approximately 10 mm × 10 mm), 2. one-twentieth Gliadel wafer, and 3. HSNM (10 mm × 10 mm) surgically implanted onto the brain surface of rats. (b) F98 cells expressed approximately seven times higher levels of MGMT than 9L cells. (c) *In vivo* release curve for O^6-BG, BiCNU, and TMZ liberation from the HSNMs.

kg body weight). A scalp cut was performed at the right postorbital area. The galea overlying the right cranium was swept laterally, and craniectomy (around 1 cm × 1 cm) was created using an electric burr (Figure 1(a), panel 1). The rats were guarded in a stereotactic rack (Model SAS 64612; ASI Instruments, Warren, MI) after meticulous hemostasis. All 150 rats were randomly divided into two groups, 75 were implanted with 9L cells, and the remaining 75 received F98 cells. Culture medium (10 μl) containing 2–3 × 10^5 9L or F98 cells was injected for more than 3 min through a fine needle (26-gage) inserted 3 mm in depth into the core of the craniectomy. Following glioma implantation, the rats were permitted to recover from anesthesia and were given free access to water and food.

Approximately 13–16 days following implantation of tumor cells, T1- and T2-weighted MRI images were acquired to confirm that glioma models had been successfully created. Then the tumor-bearing rats were randomly divided into groups (12–15 rats per group) based on the five treatment methods administered: oral TMZ with Gliadel wafer implantation (group A implantation of single-layer nanofibrous membrane loaded with BiCNU and TMZ (group B), intraperitoneally injected with O^6-BG 1–2 h before Gliadel wafer implantation, followed by oral TMZ (group C), HSNM implantation (group D), and no treatment (only a sham procedure of craniectomy, group E). In all groups, subgroups I and II represented F98 and 9L tumor-bearing rats (subgroup II), respectively (Table 1).

One-twentieth of a Gliadel wafer (with approximately 0.385 mg BiCNU) was placed on the brain surface (Figure 1(a), panel 2) of group A and C rats after the tumor was confirmed through MRI. Group c rats accepted O^6-BG pretreatment, the O^6-BG was intraperitoneally administered at a dosage of 50 mg/kg over 1–2 h before surgically implanting the Gliadel wafer. Oral TMZ (Temodal 100 mg) was orally administered to group A and C rats at a dosage of 200 mg/BSA (m^2) once daily for

Table 1. Rat groups.

Treatment/implanted tumor cell	I. F98	II. 9L
A. Gliadel + Oral TMZ	AI	AII
B. One-layer NM: BiCNU/TMZ	BI	BII
C. i.p. O^6-BG, Gliadel + Oral TMZ	CI	CII
D. HSNM: O^6-BG → BiCNU/TMZ	DI	DII
E. None	EI	EII

BiCNU, carmustine; HSNM, hybrid-structured nanofibrous membrane; i.p., intraperitoneal; NM, nanofibrous membrane; TMZ, Temozolomide.

Table 2. Drug dosage.

Drugs (route)		Dosage	Applied to rat
Gliadel (imp)		1/20 wafer	0.385 mg
Temozolomide (oral)		1/10 capsule	10 mg × 5 days
O^6-BG (i.p.)		50 mg/kg	12.5–15.0 mg
Nanofibers (imp)	**BiCNU**	60 mg in 100 cm^2 NM	0.384 mg
	Temozolomide	60 mg in 100 cm^2 NM	0.384 mg
	O^6-BG	12.5 mg in 100 cm^2 NM	0.125 mg

BiCNU, carmustine; imp, surgical implantation, i.p., intraperitoneal.

the first 5 days, followed by a 23-day treatment interruption (cycle 1). If the tumor-bearing rats survived longer than 1 month, cycle 2 was initiated. In group B rats, single-layer 50:50 PLGA nanofibrous membranes impregnated with TMZ and BiCNU were surgically placed onto the surface of the cerebral parenchyma. The HSNM was surgically implanted onto the cerebral surface of group D rats (Figure 1(a), panel 3). The therapeutic dosage is listed in Table 2.

MRI

Gross wound appearance was observed daily, in combination with regular brain MRI examinations. The entire MRI scanning was completed employing 7-Tesla Biospec (Bruker, Ettlingen, Germany). Prior to the treatment (approximately 13–16 days following implantation of tumor cells), T1- and T2-weighted images were acquired to prove the satisfactory formation of glioma models without epidural, subdural, or intracerebral hemorrhage, abnormal fluid accumulation, or abscess.

T2-weighted images were acquired as a reference to identify the tumor region at 0, 2, 4, 8, 12, and 16 weeks following the application of various treatment regimens. The TVs were reconstructed and calculated using commercially available software OsiriX Viewer (Bernex, Switzerland). Any new region of nonenhanced T2 or fluid-attenuated inversion recovery signal persistent with tumor growth indicates an evolutionary glioma. The treatment effectiveness was assessed by the tumor volumes based on the confirmatory MRI performed following 4 weeks of treatment.

Microscopic examination

Following 4–5 weeks of treatment, at least one rat in each test group was sacrificed for pathological examination after a follow-up MRI, and the brain tissue was gathered for pathological analysis (the sacrificed animals were removed from the survival estimation). The cerebral tissue was immersed in 10% buffered formal saline before routine embedding in paraffin and then microscopic evaluation of H&E-stained 5-μm-thick

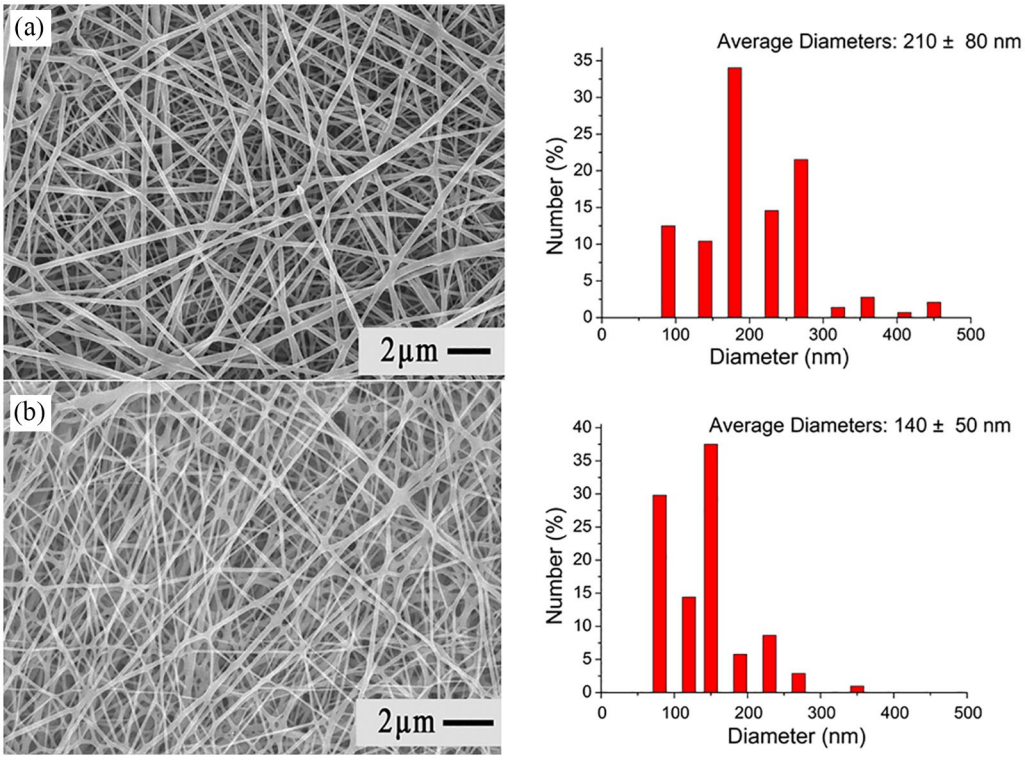

Figure 2. SEM image and fiber size distribution: (a) blend nanofibers; (b) sheath-core nanofibers.

sections. Immunocytochemical staining of antibodies against GFAP was also performed on these sections. The Ki-67 labeling index evaluated through MIB-1 immunostaining was expressed as a percentage, derived by counting the number of positively stained nuclei in 1000 tumor cells pooled from 3 to 5 fields (each 0.16 mm^2) examined at high-power magnification. Apoptosis in tissue sections was evaluated using the *in situ* terminal deoxynucleotidyl transferase-mediated dUTP-biotin nick end-labeling (TUNEL) assay.

Statistical analysis

Experimental results were expressed as mean ± standard deviation. Differences were analyzed with the paired-sample *t* test employing the Stata software (TX, USA). A *p* value of <0.05 was deemed statistically significant. Data of survival was analyzed by employing the Kaplan–Meier method, while the statistical significance was decided employing the *post hoc* log-rank test. The repeated-measures mixed model was used for assessing the influence of various therapies on the proliferation of the transplanted tumor.

Results

Assessment of HSNMs

Nanofibrous membranes were satisfactorily fabricated using the electrospinning process. Figure 2 shows the SEM images of the spun fibers and fiber size distributions. The estimated diameters were 210 ± 80 nm and 140 ± 50 nm, respectively, for blend and sheath-core nanofibers. Figure 3 shows the FTIR spectra of pure PLGA films and HSNMs. A new vibration peak at 1575–1630 cm^{-1} was detected due to the N=N bonds of TMZ. The peak at 2900–3000 cm^{-1} (CH_2 bond) was promoted with the incorporation of BiCNU. Meanwhile, the new peak at 3300–3500 cm^{-1} was attributable to the N-H bond of BiCNU. In addition, the vibration near 650–900 cm^{-1} could be attributable to the NH_2 bond of O^6-BG. The FTIR spectra assay confirmed that the pharmaceuticals were successfully embedded in the PLGA membranes.

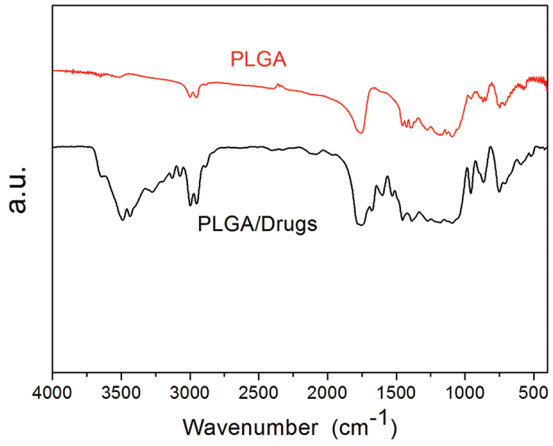

Figure 3. FTIR spectra of pure PLGA nanofibrous membranes and HSNMs. The spectra assay confirmed that the pharmaceuticals were successfully embedded in the PLGA membranes.

MGMT expression

The authors assessed the performance of MGMT protein in F98 and 9L glioma cell lines by immunoblotting. The results revealed that F98 cells expressed levels of MGMT that were approximately seven times higher than 9L cells (Figure 1(b)).

In vivo *liberated behaviors of biopharmaceuticals from the HSNMs*

The fabricated HSNMs demonstrated a sequential drug release (Figure 1(c)), with the liberation of high O^6-BG concentrations in the early phase, followed by high levels of TMZ and BiCNU for 3–4 weeks. The concentrations of O^6-BG, BiCNU, and TMZ remained high for over 14 weeks in the brain tissues of the rats. Systemic (blood) drug concentration was significantly lower than the local (cerebral parenchyma) drug concentration. The differences at each time-point were significant ($p < 0.05$).

MRI and TV

Approximately 13–16 days after implanting F98 or 9L tumor cells into rat brains, the authors confirmed the creation of the glioma models through T1- and T2-weighted imaging. The animals that expired in the perioperative period (during the first three postoperative days), displayed wound infection or showed failed tumor creation were eliminated. In total, 119 glioma rats (59 F98 tumor-bearing rats and 60 9L tumor-bearing rats) were created successfully. Programmed brain MRI examination was performed at 2, 4, 6, 10, and 14 weeks following treatment. Figure 4 presents the brain MRI scans in each subgroup. In subgroup EI and EII, the tumor size increased significantly, causing a severe mass effect and midline shift. In addition, the tumors grew rapidly in subgroups AI and AII with a severe mass effect. Tumors grew more slowly in subgroups DI and DII, but the tumor size decreased, making the tumors appear smaller than those at the initial stage in subgroup DI. Figure 5 presents the whole

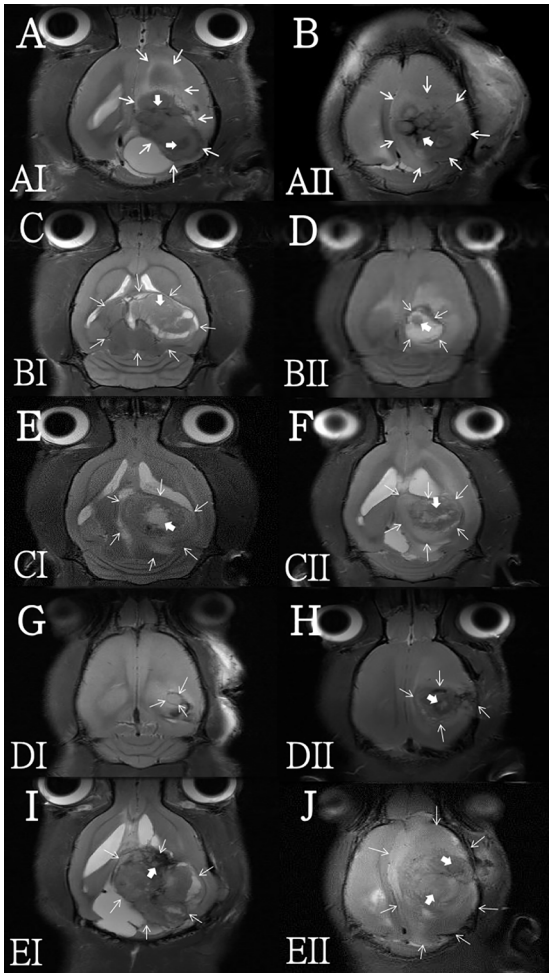

Figure 4. Brain MRI 4 weeks after treatment in each subgroup. The letters on the lower-left corner of each image indicate the subgroup. Central necrosis and tumor are indicated with thick and thin arrows, respectively. The tumor fulminant expansion caused severe mass effect and midline shift in subgroup EI I and EII J, whereas rapid growth in subgroups AI A and AII B resulted in ventricle compression and midline shift. In subgroups BI C, BII D, CI E, and CII F, tumor growth caused mild-to-moderate mass effect and midline shift. TV decreased without midline shift in subgroup DI G and there was a slight increase in subgroup DII H.

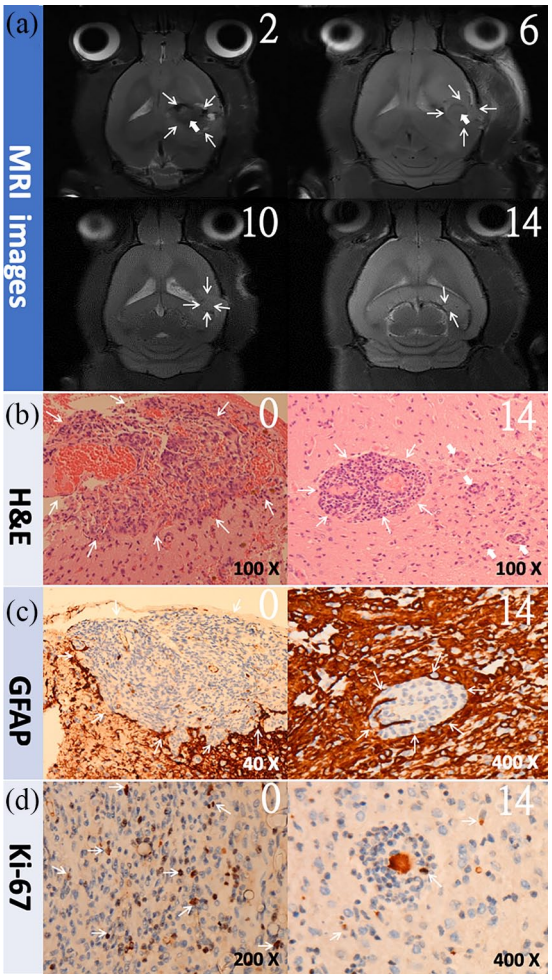

Figure 5. The study results of subgroup DI. The number on the upper-right corner indicates weeks after HSNM implantation. (a) Serial MRI scans. The tumor decreasing in size with time and no tumor regrowth was noted. (b) H&E staining image. The tumor area is restricted and localized with a low number of satellite tumor cells outside the tumor mass (thick arrows). (c) GFAP immunocytochemical staining. GFAP-positive glial cells (thin arrows) are distinct and surround the shrinking tumor. (d) The Ki-67 labeling index. Approximately 12.21% before and 4.93% 14 weeks after HSNM implantation.

course results in subgroup DI. Figure 5(a) displays serial MRI scans in subgroup DI. The TV grew and achieved its peak value approximately 2 weeks after treatment and thereafter reduced gradually. At the conclusion of the study (i.e. 14 weeks following treatment), almost no tumor was noted on the MRI scans.

TVs were rebuilt and estimated using the open-sourced imaging code (Digital Imaging and Communication in Medicine, OsiriX) approved by the Food and Drug Administration. The average TVs before treatment (approximately 13–16 days after glioma cell incubation) ranged from $74.25 \pm 21.64 \times 10^{-3}$ ml (EI) to $110.03 \pm 44.03 \times 10^{-3}$ ml (AI), with no statistical difference between any two subgroups initially. The authors compared TVs before treatment and 4 weeks after treatment for each subgroup to evaluate the growth of the implanted tumors. Figure 6(a) shows the variation in the TVs in each subgroup. In the nontreatment group, the initial TVs were $107.13 \pm 49.32 \times 10^{-3}$ and $74.25 \pm 21.64 \times 10^{-3}$ ml in subgroups EI and EII, respectively. The tumors grew rapidly, and the majority of rats died before completing 4 weeks post-treatment, with the mean TV increasing to $728.20 \pm 256.68 \times 10^{-3}$ and $637.83 \pm 267.42 \times 10^{-3}$ ml in subgroups EI and EII, respectively. In group A, a Gliadel wafer was surgically implanted in the rats, followed by oral TMZ 1 week later. In subgroup AI, the initial mean TV of $110.02 \pm 44.03 \times 10^{-3}$ ml increased to $710.25 \pm 176.17 \times 10^{-3}$ ml after 4 weeks of treatment. Similarly, in subgroup AII, the mean TV increased from $93.52 \pm 31.14 \times 10^{-3}$ ml initially to $574.37 \pm 308.95 \times 10^{-3}$ ml after 4 weeks of treatment. At 4 weeks after treatment, the mean TV was higher in subgroup AI than in subgroup AII, but without statistical significance ($p = 0.624$). Group B rats were treated with a single-layered nanofibrous membrane. In subgroups BI and BII, the mean TVs were $75.21 \pm 27.29 \times 10^{-3}$ and $74.84 \pm 26.21 \times 10^{-3}$ ml, respectively, which increased to $459.38 \pm 275.07 \times 10^{-3}$ and $444.49 \pm 167.66 \times 10^{-3}$ ml 4 weeks after treatment, respectively. However, the difference was not significant. Although the mean TVs in subgroups BI and AI were significantly different ($p = 0.016$), those in subgroups BII and AII were not ($p = 0.810$; Figure 6(b)). In group C, the rats were treated with O^6-BG 1–2 h before surgically implanting a Gliadel wafer, followed by oral TMZ 1 week later. The mean TVs did not differ significantly between subgroups CI and CII initially ($84.28 \pm 35.40 \times 10^{-3}$ and $78.14 \pm 48.06 \times 10^{-3}$ ml, respectively) or 4 weeks after treatment ($662.45 \pm 298.13 \times 10^{-3}$ and $472.60 \pm 324.80 \times 10^{-3}$ ml, respectively). In addition, the mean TVs did not differ significantly between subgroups CI and BI, CII and BII, CI and AI, or CII and AII. In group D, the HSNMs were surgically implanted in tumor-bearing rats and the initial mean TVs was $89.88 \pm 19.00 \times 10^{-3}$ and $82.04 \pm 18.16 \times 10^{-3}$ ml in subgroups DI and

DII, respectively (the difference was not significant). In subgroup DI, the mean TVs gradually increased within 2 weeks of HSNM implantation. The mean TV of $104.93 \pm 73.42 \times 10^{-3}$ ml 2 weeks after treatment decreased to $88.08 \pm 117.64 \times 10^{-3}$ ml 4 weeks after treatment. In contrast, in subgroup DII, the mean TV increased gradually to $241.13 \pm 67.17 \times 10^{-3}$ ml 2 weeks after HSNM implantation and then to $346.66 \pm 113.19 \times 10^{-3}$ ml 4 weeks after HSNM implantation. The differences in TVs between subgroups DI and CI (Figure 6(c)), DI and BI (Figure 6(d)), and DI and DII (Figure 6(e)) were significant ($p < 0.05$), but those between subgroups DII and CII (Figure 6(c) and DII and BII (Figure 6(d)) were not significant ($p > 0.05$).

Survival analysis

After excluding the 10 tumor-bearing rats that weresacrificed for pathological examination, 11, 10, 10, 10, 11, 10, 13, 12, 11, and 11 rats were included in subgroups AI, AII, BI, BII, CI, CII, DI, DII, EI, and EII for survival analysis, respectively. Figure 7(a) presents the Kaplan–Meier curves of a typical survival study in each subgroup. In control group E, the median survival time was 35.45 ± 11.33 and 39.18 ± 13.33 days in subgroups EI and EII, respectively, but the difference was not significant ($p = 0.455$). In addition, the median survival time was 51.27 ± 15.62 and 55.10 ± 20.04 days in subgroups AI and AII, respectively, without statistical significance ($p = 0.715$), but it was 59.90 ± 19.19 and 63.00 ± 16.97 days in subgroups BI and BII, respectively. Although the discrepancies in the median survival time between subgroups BI and BII as well as BI and AI were not significant, those between BII and AII were ($p = 0.039$; Figure 7(b)). In group C, the survival time was 63.00 ± 16.97 and 68.91 ± 16.02 days in subgroup CI and CII, respectively. No significant difference was found in the survival times between subgroups CI and CII, CI and BI, as well as CII and BII. In contrast, the median survival time was significantly different between subgroups CI and AI as well as CII and AII (Figure 7(c)). The mean survival time was significantly shorter in subgroup DII (70.83 ± 16.49 days) than that in subgroup DI (90.46 ± 14.91 days; $p < 0.05$; Figure 7(e)). Moreover, the median survival time was significantly different between subgroups DI and CI ($p = 0.001$), but not between DII and CII ($p = 0.420$; Figure 7(d)).

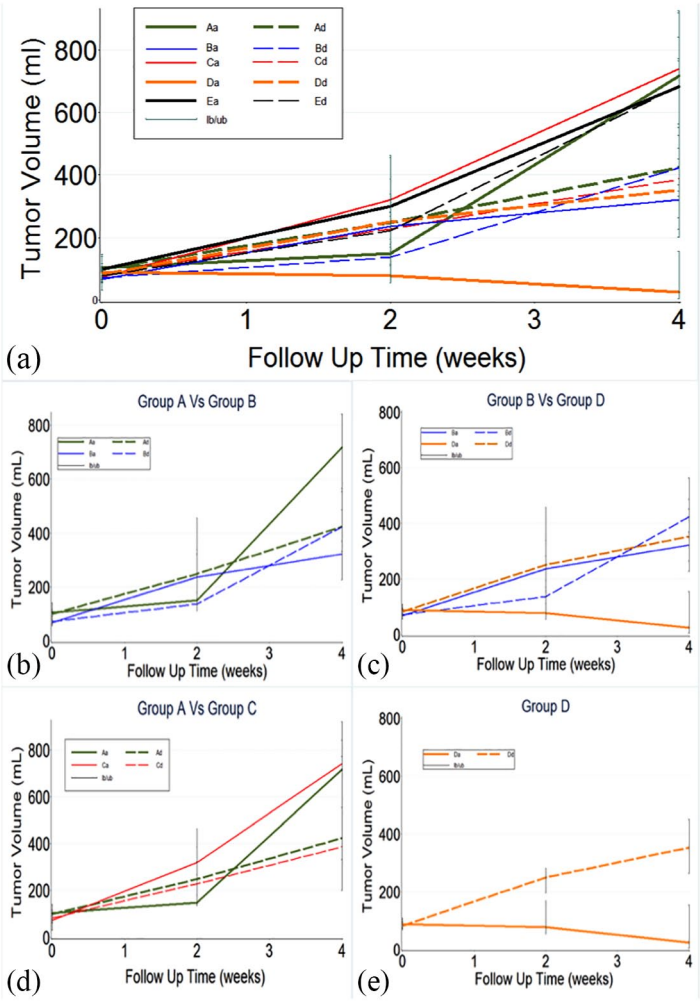

Figure 6. The repeated-measures mixed model was used to evaluate differences in the mean 4-week TVs between each subgroup. (a) TVs increased at various rates, except in group DI. The TV decreased after HSNM implantation. (b) TVs were significantly different between subgroups BI and AI ($p = 0.016$), but not between subgroups BII and AII ($p = 0.810$). (c) and (d) TVs were significantly different between subgroups DI and CI as well as DI and BI ($p < 0.05$), but not between subgroups DII and CII as well as DII and BII ($p > 0.05$). (e) TVs were significantly different between subgroups of DI and DII ($p < 0.001$).

Pathology

Figure 8 illustrates the H&E staining results for each subgroup. Subgroups EI, EII, AI, AII, and CII revealed diffused karyorrhectic tumor cells, covering a large area, with either coagulation necrosis, or microvascular proliferation with thick vascular walls. In addition, considerable serpiginous necrosis with palisading near the necrotic foci was detected. Subgroups BI, CI, CII, DI, and DII demonstrated considerable multinucleated tumor cells with restricted area, but with minor pseudopalisading necrosis and

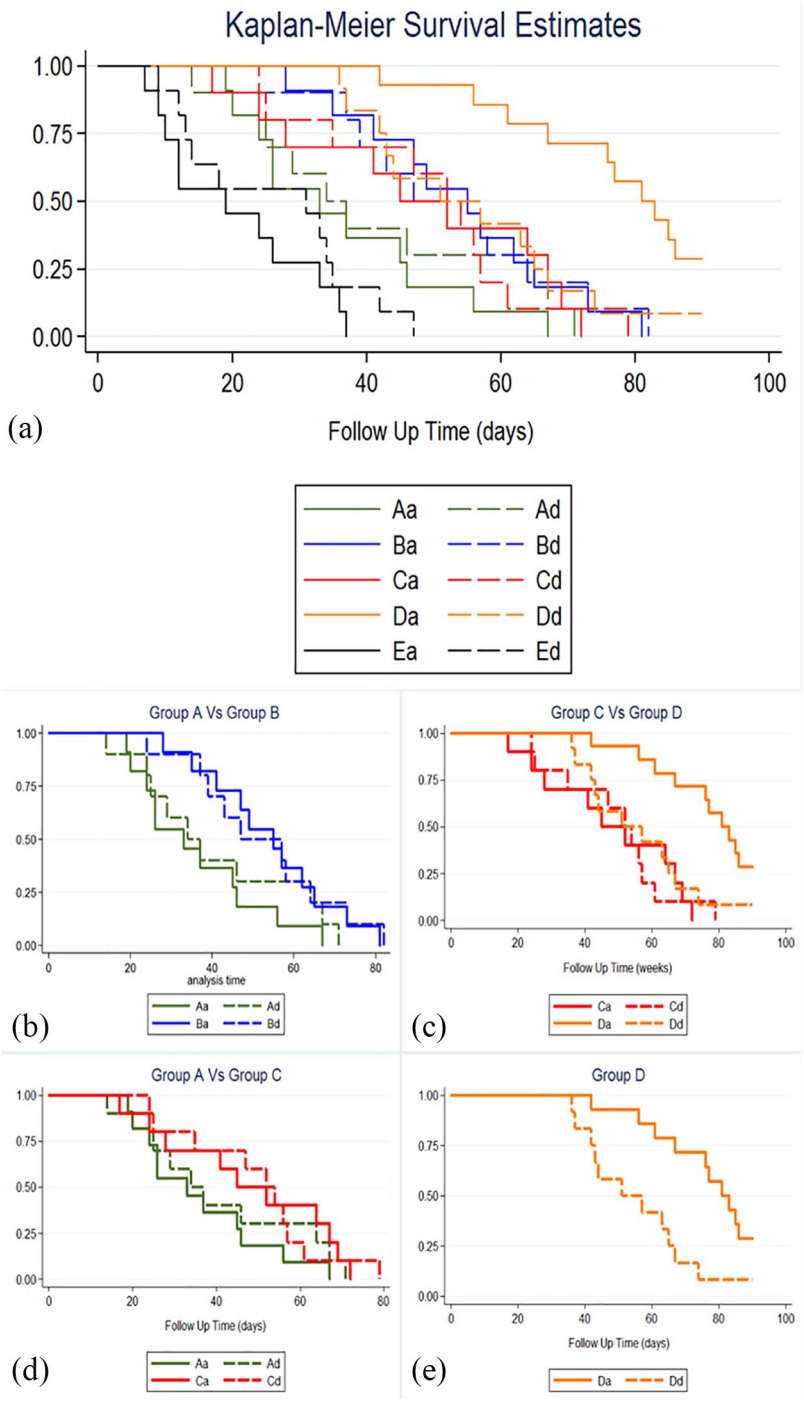

Figure 7. Overall survival of tumor-bearing rats in each subgroup. (a) Of the five groups, group D had the longest survival time, followed by groups B, C, A, and E. (b) The survival time was significantly different between subgroups BII and AII ($p = 0.039$). (c) The survival time was significantly different between subgroups CI and AI as well as CII and AII. (d) The survival time was significantly different between subgroups DI and CI ($p = 0.001$), but not between subgroups DII and CII ($p = 0.420$). (e) The survival time was significantly shorter in subgroup DII than in subgroup DI ($p < 0.05$).

endothelial proliferation. The tumor area was obviously reduced and restricted in subgroups DI and DII. Figure 5(b) illustrates H&E staining images before and after14 weeks of treatment in subgroup DI. The tumor area was restricted and localized with few satellite tumor cells outside

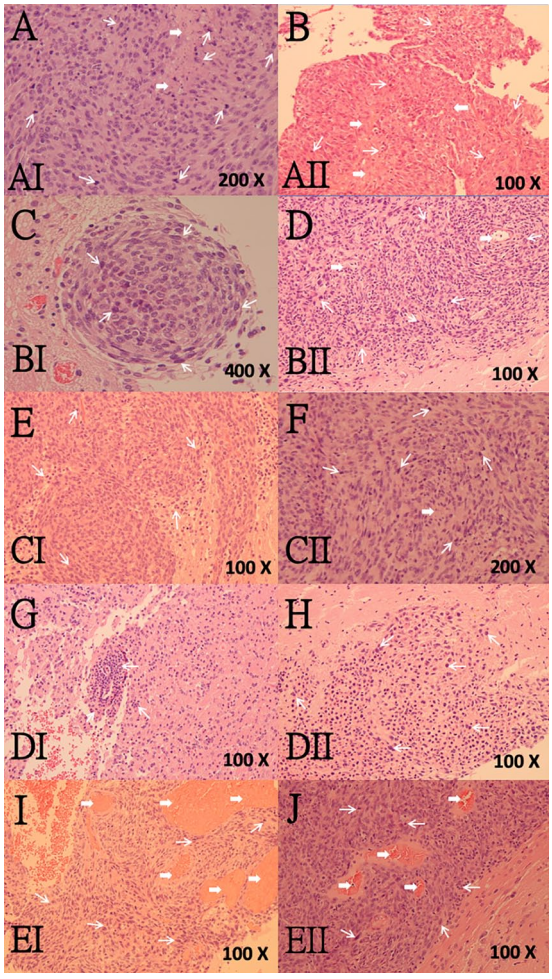

Figure 8. H&E staining. The letters in the lower-left corner of each image indicate the subgroup. Karyorrhectic tumor cells and central (coagulation) necrosis are indicated with thin and thick arrows, respectively. Diffuse karyorrhectic tumor cells with central necrosis were noted in subgroups EI I, EII J, AI A, AII B, and BII D. Restricted tumor area and little central necrosis were observed in subgroups BI C, CI E, and CII F. The tumor cells tended to localize in small areas in subgroups DI G and DII H.

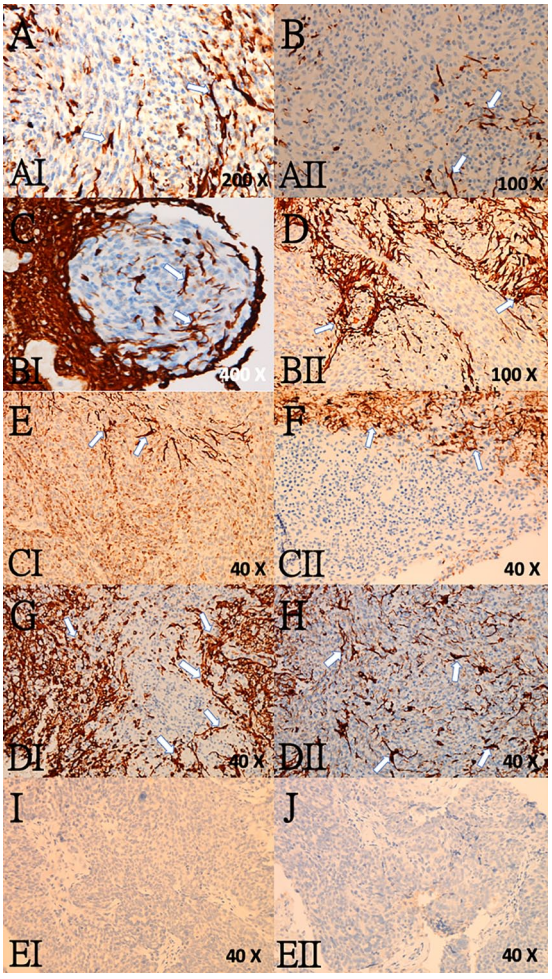

Figure 9. GFAP immunocytochemical staining. The letters in the lower-left corner of each image indicate the subgroup. GFAP-positive glial cells are indicated with arrows. No GFAP expression was noted in subgroups EI I and EII j. A small number of scattered GFAP-positive glial cells were detected in subgroups AI A, AII B, and CI E. A number of scattered GFAP-positive glial cells were detected in subgroups BI C, BII D, and CII F. Coarse, dendritic GFAP-positive glial cells were detected in subgroups DI G and DII H.

major tumor clusters. Immunocytochemical staining of cytoplasmic processes for glial fibrillary acidic protein (GFAP) is illustrated in Figure 9. No GFAP-positive immunoreactivity was detected in the tumor cells in subgroups EI and EII. However, a few thin GFAP-positive glial cells were detected in the intratumor area in subgroups AI, AII, CI, and CII, but subgroups BI and BII exhibited several, thick GFAP-positive glial cells in the intratumor area. The highest number of GFAP-positive intratumor glial cells were observed in subgroups DI and DII, these cells showed dendrites. As shown in Figure 5(c) GFAP expression was sparsely distributed before treatment because the tumor shrank the coarse GFAP-positive glial cells as well as the surrounding and lobulated the tumors. The intratumor GFAP-positive glial cells remained rare. Figure 10 presents the Ki-67 labeling index in each subgroup. MIB-1 immunoactivity illustrated a proliferation of up to $13.6\% \pm 4.97\%$ before treatment. The Ki-67 labeling index was the highest in subgroups EI ($77.92\% \pm 3.94\%$) and EII ($80.24\% \pm 10.24\%$). The Ki-67 labeling index was $49.43\% \pm 2.18\%$, $35.42\% \pm 7.69\%$, $42.42\% \pm 5.18\%$, and $39.43\% \pm 5.56\%$ in

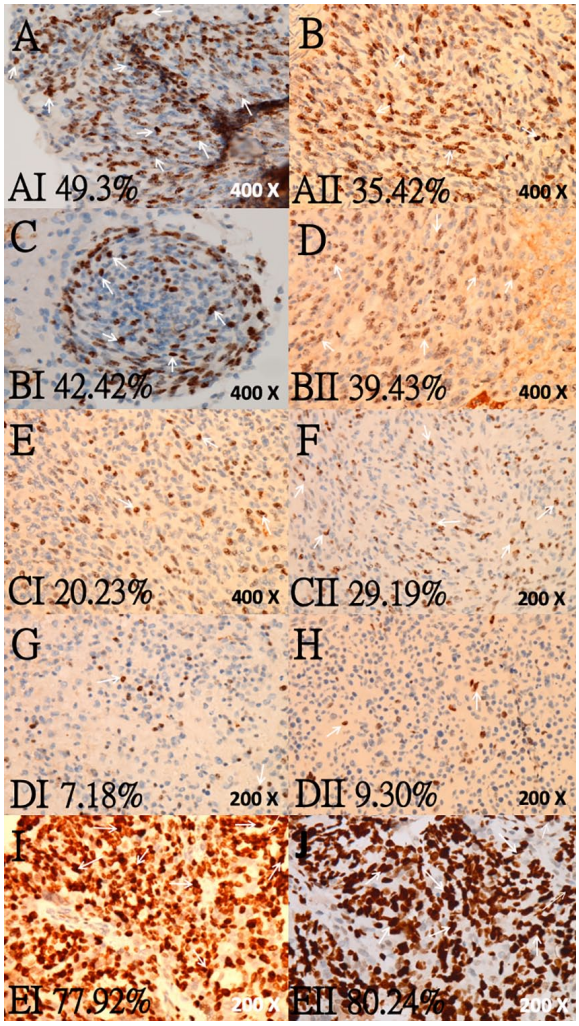

Figure 10. The Ki-67 labeling index by MIB-1 immunostaining in each subgroup. The letters in the lower-left corner of each image indicate the subgroup, followed by its Ki-67 labeling index (percentage). The arrows indicate Ki-67-positive cells. An extremely high Ki-67 labeling index was detected in subgroups EI I and EII J. The Ki-67 labeling index in subgroups AI A, AII B, BI C, and BII D was 49.43%, 35.42%, 42.42%, and 39.43%, respectively. The Ki-67 labeling index was low in subgroup CI E (approximately 20.73%) and was 29.19% in subgroup CII F. The Ki-67 labeling index decreased to less than 10% in subgroups DI G and DII H.

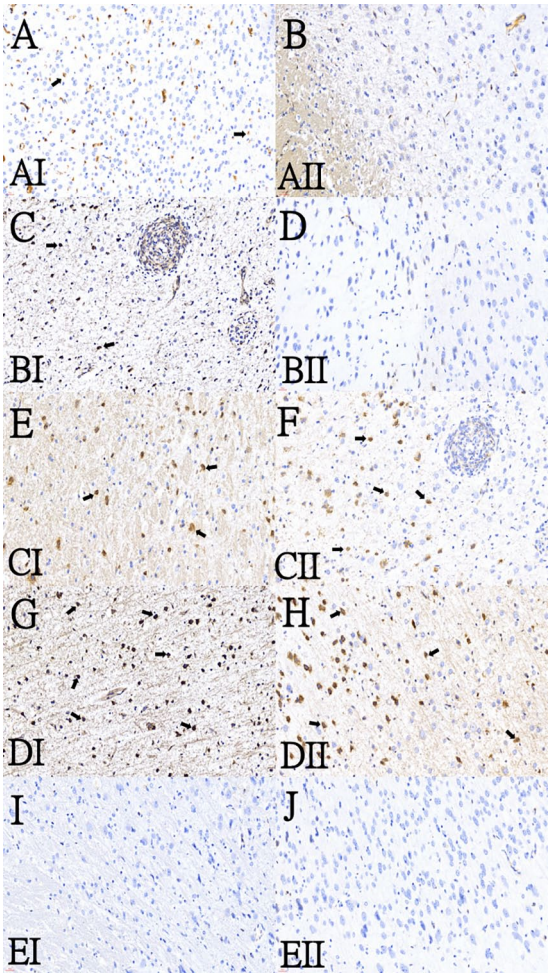

Figure 11. Evaluation of apoptosis of glioma cells by TUNEL assay in each subgroup. The letter at the lower-left corner of each image denotes the subgroup, while the black arrows indicate TUNEL-positive apoptotic cells. A limited number of apoptotic nuclei were found in subgroups AI A, AII B, BI C, and BII D, but subgroups CI E and CII F displayed some apoptotic nuclei in the intratumor area. A significant increase in the number of TUNEL-positive apoptotic nuclei was observed in subgroups DI G and DII H. However, no TUNEL-positive apoptotic nucleus were detected in the tumor cells in subgroups EI I and EII J. (Magnification, 100×).

subgroups AI, AII, BI, and BII, respectively, with no statistically significant difference among the various subgroups. The Ki-67 labeling index was considerably lower in group C than in groups A and B. The estimated Ki-67 labeling index was $20.73\% \pm 2.77\%$ and $29.19\% \pm 4.70\%$ in subgroups CI and CII, respectively. In subgroups DI and DII, the Ki-67 labeling index decreased following therapy and was significantly lower than that before therapy ($p < 0.05$). The Ki-67 labeling index was $7.18\% \pm 1.71\%$ and $9.30\% \pm 3.25\%$ in subgroups DI and DII, respectively. Figure 5(d) demonstrates that the Ki-67 labeling index was approximately 12.21% before HSNM implantation, decreasing to 4.93% 14 weeks after implantation. Apoptosis of glioma cells was evaluated by TUNEL assay and the results are illustrated in Figure 11. The highest numbers of TUNEL-positive apoptotic nuclei were observed in subgroups DI and DII, these

cells were stained dark brown. No TUNEL-positive apoptotic nucleus was detected in the tumor cells in subgroups EI and EII. However, a limited number of apoptotic nuclei were found in subgroups AI, AII, BI, and BII, whereas subgroups CI and CII displayed some apoptotic nuclei in the intratumor area.

Discussion

Intravenous and oral treatment is generally less costly and well tolerated when compared with neurosurgical drug administration. However, chemotherapeutics impair healthy cerebral tissues, leading to adverse effects and systemic toxicity, greatly limiting their maximum tolerated dose, and thus, their therapeutic efficacy. O^6-BG, which is inert and nontoxic when systemically administered alone, exhibits toxicity and adverse effects when employed as a pretreatment before systemic BiCNU or TMZ therapy.[12] In animal models with MGMT-active (nonmethylated) BiCNU-resistant tumors, MGMT activity is inhibited for several hours following exposure to O^6-BG, during which tumors become highly sensitive to BiCNU.[15] When both O^6-BG and BiCNU are administered systemically, although O^6-BG promotes BiCNU activity, it also enhances its hematopoietic toxicity.[22] Early phase studies have demonstrated that O^6-BG/TMZ administration causes severe off-target myelosuppression. In a study 46% of patients administered TMZ at the maximum tolerated dose (472 mg/m^2) in combination with O^6-BG exhibited grade 4 neutropenia.[5,23] Notably, the maximum effective alkylating agent dose in combination with O^6-BG is restricted by the systemic toxicity of O^6-BG. The systemic toxicity caused by MGMT inhibitors could be prevented by using a local delivery system. In a trial, Konck and colleagues[24] locally administered O^6-BG using an Ommaya reservoir with concomitant oral TMZ. Whether local O^6-BG administration causes MGMT inhibition in the residual tumor requires confirmation. However, this trial demonstrated that intracerebral O^6-BG treatment with concomitant TMZ (or potentially any other alkylating agent) might be an improved strategy for glioma therapy.[24] In a phase I trial, Weingar and colleagues[21] demonstrated that systemic O^6-BG can be concurrently used with intracranially transplanted BiCNU wafers with no extra toxicity. In a phase II trial, Quinn and colleagues[25] demonstrated that the effectiveness of implanted Gliadel wafers may be enhanced with the addition of O^6-BG. In addition, Rhines and colleagues [12] concluded in their clinical trial that O^6-BG can promote the effects of interstitially transported BiCNU, particularly for MGs with high MGMT expression.

Progresses in personalized medicine and drug delivery have generated a large number of opportunities in oncology. Nevertheless, approximately 98% of the examined drugs could not penetrate the BBB, mainly because of their molecular or physicochemical properties.[26] The BBB restricts the delivery of a chemotherapeutic agent inside a brain tumor, even at toxic systemic levels.[7,27] Nanomaterials have long been proposed as carriers to promote the entry and delivery of therapeutic agents into the brain.[7,28,29] PLGA-based nanoparticles are currently being investigated for applications in cancer imaging and therapy.[30–32] The two monomers of PLGA, LA, and GA, are endogenous and can be readily metabolized by the body through the Krebs cycle.[26,31] PLGA possesses a wide range of degradation rates, governed by the composition of chains, and it provides superior control to the combination of its monomers, even at varying ratios. The methyl side groups inside PLA cause the material to be more hydrophobic than PGA. LA-rich PLGA is less hydrophobic, absorbs less water, and degrades more gradually than GA-rich PLGA.[33,34] However, PLGA with a 50:50 monomers ratio can degrade rapidly and be entirely resorbed within approximately 2 months.[34]

A number of novel therapeutic approaches have been introduced to prevent chemoresistance. The concurrent use of a combination (or cocktail) of special groups of biopharmaceutical agents, including a combination of chemotherapeutic and antiangiogenic agents, cytotoxins and gene therapy;[7,15] except in rare cases, monotherapy has had limited success in treating human malignancies compared with multidrug therapy.[9] Increasing therapeutic concentrations in target areas to promote therapeutic effects and prevent tumor resistance.[32,35] Previous studies have demonstrated that BiCNU-resistant human glioma cells can be readily eliminated at a drug dose of 250 μM (53.75 μg/ml).[35] Prolonging the treatment time,[27,32] in a study *in vivo* pharmacodynamics, demonstrated that the HSNMs liberated high O^6-BG concentrations in the first 2 weeks, then TMZ and BiCNU were sequentially released. Antecedently liberated O^6-BG restored tumor cell sensitivity to alkylating agents, accompanied high local BiCNU and TMZ concentrations,

improved therapeutic efficacy, and reduced drug resistance.

Gliadel wafers, employing polyanhydride as the transport vehicle, deliver a single chemotherapy agent (BiCNU) to the brain cavity. Pharmacological studies have shown that Gliadel wafers release the majority of the drug during the first 5–7 days after implantation.[20,36] In this current work, the three biopharmaceutical agents were loaded into PLGA materials and were locally delivered at high target (brain) and low systemic (blood) concentrations for more than 14 weeks. Local drug delivery abated the systemic toxicity, but the prolonged treatment time enhanced therapeutic efficacy along with diminished drug resistance.

Belanich and colleagues[37] reported that in 167 patients treated with BiCNU for MG, low tumor MGMT content was associated with enhanced survival and a prolonged period of treatment failure, but patients with higher MG MGMT expressions exhibited worse prognosis. In the present study, 9L (with one-seventh lower MGMT expression) tumor-bearing rats demonstrated longer median survival rates, slower tumor growth, and lower malignancy than F98 (higher MGMT expression) tumor-bearing rats. In subgroups EI, AI, and CI, the mean TVs 4 weeks after treatment were greater than those in subgroups EII, AII, and CII, respectively ($p = 0.922$, 0.624, and 0.172, respectively). Similarly, in subgroups EI and AI, the median survival time was shorter than that in subgroups EII and AII, respectively ($p = 0.455$ and 0.715, respectively). Thus, tumor-bearing rats with high MGMT expression had relatively poorer outcomes. In group C, O^6-BG (50 mg/kg) was intraperitoneally injected approximately 1–2 h before implanting a Gliadel wafer, followed by 5-day oral TMZ 1 week later. However, one bolus injection of O^6-BG could not reverse high MGMT expression in tumor-bearing rats. This treatment result was similar to that of group B. In group D, the rats were treated with multidrug-loaded HSNMs, which sustainably released O^6-BG, followed by TMZ and BiCNU, for 14 weeks. The median survival time was significantly longer in subgroup DI than in DII ($p < 0.05$). Moreover, the mean TVs 4 weeks after treatment were greater in subgroup DII than in DI ($p < 0.001$).

Treatment with an intraperitoneal injection of O^6-BG 2 h before implanting BiCNU polymer can considerably enhance the efficacy of nitrosourea. However, O^6-BG administered 24 h before implanting a BiCNU wafer did not affect BiCNU sensitivity.[12,38] This is likely the resynthesis outcome of cytoprotective levels of MGMT before BiCNU administration.[12,15] In the current study, the continual and sustainable interstitial O^6-BG administration had considerable therapeutic benefits. In group B, the tumor-bearing rats were treated with single-layer nanofibrous membranes loaded with TMZ and BiCNU. In subgroups BI and BII, the median survival time was significantly longer than that in subgroups AI and AII ($p = 0.247$ and 0.039, respectively), whereas the mean TVs 4 weeks after treatment were lower than those in subgroups AI and AII ($p < 0.05$ and $p = 0.810$, respectively). The outcomes demonstrated that continual and prolonged alkylating agent treatment strengthened therapeutic efficacy. In addition, the treatment outcomes (survival time and TV) of group B and C did not significantly differ, indicating that one bolus injection of O^6-BG does not enhance the therapeutic efficacy of alkylating agents.

MG and anaplastic astrocytoma arise from astroglial cells. The number of cells expressing GFAP is inversely proportional to the extent of anaplasia.[27,39] The loss of GFAP repression could be a step in MG and anaplastic astrocytoma development and progression.[39,40] The Ki-67 labeling index has been widely used as an indicator of cell proliferation in glioma. Overexpression of Ki-67 can predict poor prognosis of glioma patients because an increase in the Ki-67 labeling index value is associated with an increasing grade of malignancy.[41,42] Group E demonstrated no GFAP-positive glial cells, but group D did, particularly in subgroup DI. The Ki-67 labeling index was extremely high in the nontreatment group and low in groups B and C, while the index in group D decreased to less than that before treatment. A significant increase in the numberof TUNEL-positive apoptotic cells was observed in tumor (tissue) sections of the HSNMs-treated group. The results of GFAP expression, Ki-67 labeling index, and TUNEL assays were in accordance with survival rate and tumor growth.

The fabricated HSNMs could perform combination therapy (gene therapy with two alkylating agent administration), target therapy (local drug concentration was higher than systemic drug concentration), and sustainable delivery (for more than 14 weeks). In addition, the biodegradable

membranes conformed satisfactorily to the geometry of the brain tissue and entirely covered the brain parenchyma, achieving effective drug transport, and eventually degraded to water and carbon dioxide, with no interference with the normal functioning of the brain.

MGs are tumors highly resistant to chemotherapy, with limited treatment alternatives. The biodegradable HSNMs sequentially and sustainably delivered high concentrations of O^6-BG, BiCNU, and TMZ for more than 14 weeks. The tumor-bearing rats treated with HSNMs demonstrated therapeutic advantages in terms of retarded and restricted tumor growth, prolonged survival time, and attenuated malignancy. The authors' findings suggest that O^6-BG potentiates the effects of interstitially transported BiCNU and TMZ. Therefore, O^6-BG may be required for the alkylating agents to offer maximum therapeutic benefits for the treatment of MGMT-expressing tumors. In addition, the HSNM-supported chemoprotective gene therapy enhanced chemotherapy tolerance and efficacy, therefore it can potentially provide an improved alternative to current therapeutic options for MGs.

Despite the proved efficacy of HSNM in treating MGs, there are limitations associated with this study. The authors divided the animals into cohorts and considered simultaneously three drugs, two different nanofibrous delivery vehicles, and three different delivery routes (surgical, oral and intraperitoneal). This makes it difficult to specifically identify which variables result in increased survival. Another limitation of the present study lies in that the relevance of the author's findings to humans with MGs remains unclear. All these will be the topics in the author's future studies.

Conclusion

MGs are tumors highly resistant to chemotherapy, with limited treatment alternatives. The biodegradable HSNMs sequentially and sustainably delivered high concentrations of O^6-BG, BiCNU, and TMZ for more than 14 weeks. The tumor-bearing rats treated with HSNMs demonstrated therapeutic advantages in terms of retarded and restricted tumor growth, prolonged survival time, and attenuated malignancy. The authors' findings suggested that O^6-BG potentiates the effects of interstitially transported BiCNU and TMZ. Therefore, O^6-BG may be required for the alkylating agents to offer maximum therapeutic benefits for the treatment of MGMT-expressing tumors. Furthermore, the HSNM-supported chemoprotective gene therapy enhanced chemotherapy tolerance and efficacy. Therefore, it can potentially provide an alternative to current therapeutic options for MGs.

Acknowledgments

We thank the staff at the 7T animal MRI Core Lab of Neurobiology and Cognitive Science Center, National Taiwan University for their technical and facility support. The editing of this manuscript by Wallace Academic Editing was also acknowledged.

Funding

This work was supported by the National Science Council of Taiwan (Contract No. NSC106-2314-B-038-045-MY2) and Chang Gung Memorial Hospital (Contract No. CMRPD2G0252).

Conflict of interest statement

The authors declare no conflicts of interest in preparing this article.

ORCID iD

Yuan-Yun Tseng https://orcid.org/0000-0003-4968-3298

References

1. Wen PY and Kesari S. Malignant gliomas in adults. *N Engl J Med* 2008; 359: 492–507.
2. Wong ET, Hess KR, Gleason MJ, *et al.* Outcomes and prognostic factors in recurrent glioma patients enrolled onto phase II clinical trials. *J Clin Oncol* 1999; 17: 2572–2578.
3. Stummer W, Reulen HJ, Meinel T, *et al.* Extent of resection and survival in glioblastoma multiforme: identification of and adjustment for bias. *Neurosurgery* 2008; 62: 564–576; discussion -76.
4. Bobola MS, Tseng SH, Blank A, *et al.* Role of O^6-methylguanine-DNA methyltransferase in resistance of human brain tumor cell lines to the clinically relevant methylating agents temozolomide and streptozotocin. *Clin Cancer Res* 1996; 2: 735–741.
5. Quinn JA, Jiang SX, Reardon DA, *et al.* Phase II trial of temozolomide plus O^6-benzylguanine in adults with recurrent, temozolomide-resistant malignant glioma. *J Clin Oncol* 2009; 27: 1262–1267.

6. Kitange GJ, Carlson BL, Schroeder MA, *et al.* Induction of MGMT expression is associated with temozolomide resistance in glioblastoma xenografts. *Neuro Oncol* 2009; 11: 281–291.
7. Tseng YY, Kau YC and Liu SJ. Advanced interstitial chemotherapy for treating malignant glioma. *Expert Opin Drug Deliv* 2016; 13: 1533–1544.
8. Minniti G, Muni R, Lanzetta G, *et al.* Chemotherapy for glioblastoma: current treatment and future perspectives for cytotoxic and targeted agents. *Anticancer Res* 2009; 29: 5171–5184.
9. Affronti ML, Heery CR, Herndon JE II, *et al.* Overall survival of newly diagnosed glioblastoma patients receiving carmustine wafers followed by radiation and concurrent temozolomide plus rotational multiagent chemotherapy. *Cancer* 2009; 115: 3501–3511.
10. Trivedi RN, Almeida KH, Fornsaglio JL, *et al.* The role of base excision repair in the sensitivity and resistance to temozolomide-mediated cell death. *Cancer Res* 2005; 65: 6394–6400.
11. Hegi ME, Diserens AC, Gorlia T, *et al.* MGMT gene silencing and benefit from temozolomide in glioblastoma. *N Engl J Med* 2005; 352: 997–1003.
12. Rhines LD, Sampath P, Dolan ME, *et al.* O^6-benzylguanine potentiates the antitumor effect of locally delivered carmustine against an intracranial rat glioma. *Cancer Res* 2000; 60: 6307–6310.
13. Kokkinakis DM, Bocangel DB, Schold SC, *et al.* Thresholds of O^6-alkylguanine-DNA alkyltransferase which confer significant resistance of human glial tumor xenografts to treatment with 1,3-bis(2-chloroethyl)-1-nitrosourea or temozolomide. *Clin Cancer Res* 2001; 7: 421–428.
14. Pegg AE. Repair of O(6)-alkylguanine by alkyltransferases. *Mutat Res* 2000; 462: 83–100.
15. Felker GM, Friedman HS, Dolan ME, *et al.* Treatment of subcutaneous and intracranial brain tumor xenografts with O^6-benzylguanine and 1,3-bis(2-chloroethyl)-1-nitrosourea. *Cancer Chemother Pharmacol* 1993; 32: 471–476.
16. Blumenthal DT, Rankin C, Stelzer KJ, *et al.* A Phase III study of radiation therapy (RT) and O(6)-benzylguanine + BICNU versus RT and BICNU alone and methylation status in newly diagnosed glioblastoma and gliosarcoma: Southwest oncology group (SWOG) study S0001. *Int J Clin Oncol* 2015; 20: 650–658.
17. Schold SC Jr, Brent TP, von Hofe E, *et al.* O^6-alkylguanine-DNA alkyltransferase and sensitivity to procarbazine in human brain-tumor xenografts. *J Neurosurg* 1989; 70: 573–577.
18. Westphal M, Hilt DC, Bortey E, *et al.* A phase 3 trial of local chemotherapy with biodegradable carmustine (BICNU) wafers (Gliadel wafers) in patients with primary malignant glioma. *Neuro Oncol* 2003; 5: 79–88.
19. Walker MD, Green SB, Byar DP, *et al.* Randomized comparisons of radiotherapy and nitrosoureas for the treatment of malignant glioma after surgery. *N Engl J Med* 1980; 303: 1323–1329.
20. Tseng YY, Liao JY, Chen WA, *et al.* Sustainable release of carmustine from biodegradable poly[((D,L))-lactide-co-glycolide] nanofibrous membranes in the cerebral cavity: in vitro and in vivo studies. *Expert Opin Drug Deliv* 2013; 10: 879–888.
21. Weingart J, Grossman SA, Carson KA, *et al.* Phase I trial of polifeprosan 20 with carmustine implant plus continuous infusion of intravenous O^6-benzylguanine in adults with recurrent malignant glioma: new approaches to brain tumor therapy CNS consortium trial. *J Clin Oncol* 2007; 25: 399–404.
22. Quinn JA, Desjardins A, Weingart J, *et al.* Phase I trial of temozolomide plus O^6-benzylguanine for patients with recurrent or progressive malignant glioma. *J Clin Oncol* 2005; 23: 7178–7187.
23. Quinn JA, Jiang SX, Reardon DA, *et al.* Phase I trial of temozolomide plus O^6-benzylguanine 5-day regimen with recurrent malignant glioma. *Neuro Oncol* 2009; 11: 556–561.
24. Koch D, Hundsberger T, Boor S, *et al.* Local intracerebral administration of O(6)-benzylguanine combined with systemic chemotherapy with temozolomide of a patient suffering from a recurrent glioblastoma. *J Neurooncol* 2007; 82: 85–89.
25. Quinn JA, Jiang SX, Carter J, *et al.* Phase II trial of Gliadel plus O^6-benzylguanine in adults with recurrent glioblastoma multiforme. *Clin Cancer Res* 2009; 15: 1064–1068.
26. Tosi G, Costantino L, Ruozi B, *et al.* Polymeric nanoparticles for the drug delivery to the central nervous system. *Expert Opin Drug Deliv* 2008; 5: 155–174.
27. Tseng YY, Su CH, Yang ST, *et al.* Advanced interstitial chemotherapy combined with targeted treatment of malignant glioma in rats by using drug-loaded nanofibrous membranes. *Oncotarget* 2016; 7: 59902–59916.
28. Tosi G, Ruozi B and Belletti D. Nanomedicine: the future for advancing medicine and

neuroscience. *Nanomedicine (Lond)* 2012; 7: 1113–1116.

29. Song E, Gaudin A, King AR, *et al*. Surface chemistry governs cellular tropism of nanoparticles in the brain. *Nat Commun* 2017; 8: 15322.
30. Danhier F, Ansorena E, Silva JM, *et al*. PLGA-based nanoparticles: an overview of biomedical applications. *J Control Release* 2012; 161: 505–522.
31. Barbu E, Molnar E, Tsibouklis J, *et al*. The potential for nanoparticle-based drug delivery to the brain: overcoming the blood-brain barrier. *Expert Opin Drug Deliv* 2009; 6: 553–565.
32. Tseng YY, Huang YC, Yang TC, *et al*. Concurrent chemotherapy of malignant Glioma in rats by using multidrug-loaded biodegradable nanofibrous membranes. *Sci Rep* 2016; 6: 30630.
33. Tseng YY, Yang TC, Wang YC, *et al*. Targeted concurrent and sequential delivery of chemotherapeutic and antiangiogenic agents to the brain by using drug-loaded nanofibrous membranes. *Int J Nanomedicine* 2017; 12: 1265–1276.
34. Makadia HK and Siegel SJ. Poly lactic-co-glycolic acid (PLGA) as biodegradable controlled drug delivery carrier. *Polymers (Basel)* 2011; 3: 1377–1397.
35. Bodell WJ, Bodell AP and Giannini DD. Levels and distribution of BICNU in GBM tumors following intratumoral injection of DTI-015 (BICNU-ethanol). *Neuro Oncol* 2007; 9: 12–19.
36. Brem H and Gabikian P. Biodegradable polymer implants to treat brain tumors. *J Control Release* 2001; 74: 63–67.
37. Belanich M, Pastor M, Randall T, *et al*. Retrospective study of the correlation between the DNA repair protein alkyltransferase and survival of brain tumor patients treated with carmustine. *Cancer Res* 1996; 56: 783–788.
38. Wedge SR, Porteous JK and Newlands ES. Effect of single and multiple administration of an O^6-benzylguanine/temozolomide combination: an evaluation in a human melanoma xenograft model. *Cancer Chemother Pharmacol* 1997; 40: 266–272.
39. Wilhelmsson U, Eliasson C, Bjerkvig R, *et al*. Loss of GFAP expression in high-grade astrocytomas does not contribute to tumor development or progression. *Oncogene* 2003; 22: 3407–3411.
40. Toda M, Miura M, Asou H, *et al*. Cell growth suppression of astrocytoma C6 cells by glial fibrillary acidic protein cDNA transfection. *J Neurochem* 1994; 63: 1975–1978.
41. Wakimoto H, Aoyagi M, Nakayama T, *et al*. Prognostic significance of Ki-67 labeling indices obtained using MIB-1 monoclonal antibody in patients with supratentorial astrocytomas. *Cancer* 1996; 77: 373–380.
42. Johannessen AL and Torp SH. The clinical value of Ki-67/MIB-1 labeling index in human astrocytomas. *Pathol Oncol Res* 2006; 12: 143–147.